THE JOURNAL OF BIOLOGICAL CHEMISTRY VOL. 291, NO. 41, pp. 21571–21583, October 7, 2016


# Homo- and Heterotypic Association Regulates Signaling by the SgK269/PEAK1 and SgK223 Pseudokinases*[S]

Received for publication, July 17, 2016, and in revised form, August 15, 2016 Published, JBC Papers in Press, August 16, 2016, DOI 10.1074/jbc.M116.748897

**Ling Liu[‡1], Yu Wei Phua[‡], Rachel S. Lee[‡], Xiuquan Ma[‡], Yiping Jenkins[‡], Karel Novy[‡], Emily S. Humphrey[§2], Howard Chan[‡], Robert Shearer[§3], Poh Chee Ong[‡], Weiwen Dai[¶‖4], Darren N. Saunders[§**5], Isabelle S. Lucet[¶‖6,7], and Roger J. Daly[‡7,8]**

*From the [‡]Cancer Program, Biomedicine Discovery Institute and Department of Biochemistry and Molecular Biology, Level 1, Building 77, Monash University, Clayton, Victoria 3800, the [§]Cancer Research Program, The Kinghorn Cancer Centre, Garvan Institute of Medical Research, 384 Victoria Street, Sydney, New South Wales 2010, [¶]The Walter and Eliza Hall Institute of Medical Research, Parkville, Victoria 3052, the [‖]Department of Medical Biology, University of Melbourne, Parkville, Victoria 3050, and the **School of Medical Sciences, University of New South Wales, Sydney, New South Wales 2052, Australia*

**SgK269/PEAK1 is a pseudokinase and scaffolding protein that plays a critical role in regulating growth factor receptor signal output and is implicated in the progression of several cancers, including those of the breast, colon, and pancreas. SgK269 is structurally related to SgK223, a human pseudokinase that also functions as a scaffold but recruits a distinct repertoire of signaling proteins compared with SgK269. Structural similarities between SgK269 and SgK223 include a predicted α-helical region (designated CH) immediately preceding the conserved C-terminal pseudokinase (PK) domain. Structure-function analyses of SgK269 in MCF-10A mammary epithelial cells demonstrated a critical role for the CH and PK regions in promoting cell migration and Stat3 activation. Characterization of the SgK269 "interactome" by mass spectrometry-based proteomics identified SgK223 as a novel binding partner, and association of SgK269 with SgK223 in cells was dependent on the presence of the CH and PK domains of both pseudokinases. Homotypic association of SgK269 and SgK223 was also demonstrated and exhibited the same structural requirements. Further analysis using pulldowns and size-exclusion chromatography underscored the critical role of the CH region in SgK269/SgK223 association. Importantly, although SgK269 bridged SgK223 to Grb2, it was unable to activate Stat3 or efficiently enhance migration in SgK223 knock-out cells generated by CRISPR/Cas9. These results reveal previously unrecognized interplay between two oncogenic scaffolds and demonstrate a novel signaling mechanism for pseudokinases whereby homotypic and heterotypic association is used to assemble scaffolding complexes with distinct binding properties and hence qualitatively regulate signal output.**

Protein kinases regulate diverse cellular processes, including proliferation, survival, metabolism, and motility. Reflecting their pleiotropic effects, they play critical roles in normal development, as well as particular human pathologies (1). Interestingly, ~10% of annotated human protein kinases lack at least one of the conserved amino acid motifs predicted to be essential for catalytic function, leading to their classification as pseudokinases (1–3). Emerging evidence indicates that pseudokinases function as allosteric regulators and/or scaffolds, rather than protein kinases capable of catalyzing phosphoryl transfer (2–4).

Among the protein kinase superfamily, dimerization, or multimerization, represents an important regulatory mechanism that can occur in a homotypic or heterotypic fashion and impacts upon kinase activation and/or signaling potential (5, 6). For example, within the ErbB family of receptor tyrosine kinases, binding of particular ligands promotes the formation of specific homo- or heterodimeric receptor complexes, where one kinase domain activates the other through an allosteric mechanism involving formation of an asymmetric kinase dimer (5). In addition, because each member of this family possesses a distinct complement of recruitment sites for Src homology (SH)[9] 2 and phosphotyrosine binding (PTB) domain-containing signaling proteins, receptor dimerization allows for diversification of signaling outcomes through use of contrasting receptor combinations (7). The complexity of protein-protein interactions contributing to dimerization of protein kinases vary and can involve direct association of particular kinase or pseudokinase domains, additional domains within the protein partners, and accessory proteins, such as 14-3-3 isoforms (5, 6). Pseudokinases that utilize multimerization as a signaling mechanism include ErbB3, which heterodimerizes with and transac-

* This work was supported in part by Project Grant 1084621 from the National Health and Medical Research Council of Australia. The authors declare that they have no conflicts of interest with the contents of this article.
[S] This article contains supplemental dataset 1 and Table S1.
*The mass spectrometric raw data and spectral libraries associated with this manuscript are available from ProteomeXchange with the accession number PXD004250.*
[1] Supported by National Health and Medical Research Council ECR Fellowship 1054497.
[2] Recipient of Research Scholar Award 10/RSA/1-28 from the Cancer Institute of New South Wales and an Australian Postgraduate Award from the University of New South Wales.
[3] Supported by a Baxter Family Scholarship.
[4] Supported by the Australian Cancer Research Foundation.
[5] Supported by National Health and Medical Research Council Grant 1052963.
[6] Supported by Australian Cancer Research Foundation and by the Walter and Eliza Hall Institute.
[7] Both authors are co-senior authors.
[8] Supported by National Health and Medical Research Council Fellowship 1058540. To whom correspondence should be addressed. Tel.: 61-3-990-29301; Fax: 61-3-990-29500; E-mail: roger.daly@monash.edu.

[9] The abbreviations used are: SH, Src homology; PK, pseudokinase; PTB, phosphotyrosine binding; TCEP, tris(2-carboxyethyl)phosphine; IP, immunoprecipitate.

tivates other ErbB family members (5), and PAN3, where homodimerization via a coiled-coil region is critical to the function of the PAN2-PAN3 deadenylase complex in regulating mRNA degradation (8).

SgK269, also known as PEAK1, was first identified as a tyrosine-phosphorylated protein enriched in cell pseudopodia that acts as a key regulator of cell spreading and migration, and it promotes anchorage-independent growth and tumorigenesis in mouse xenograft models (9). It contains a pseudokinase domain at the C terminus with substitutions in the DFG motif and glycine-rich loop important for catalytic activity of *bona fide* kinases and, presumably reflecting these changes, is devoid of nucleotide binding activity (4). Upstream of the pseudokinase domain, SgK269 contains several tyrosine phosphorylation sites within consensus motifs for binding to specific SH2 or PTB domain-containing proteins. SgK269 Y1188 binds Shc1 and mediates a key switch in EGF receptor signal output over time, from mitogenic/survival signaling to that regulating morphogenesis (10). In addition, SgK269 couples to the Ras signaling pathway via Tyr-635-mediated binding to the Grb2 SH2 domain (11). Overexpression of SgK269 in mammary epithelial cells promotes a partial epithelial-mesenchyme transition and aberrant growth and morphogenesis in 3D Matrigel culture, identifying SgK269 as a potential breast cancer oncogene (11). A likely oncogenic role for this pseudokinase is further underscored by its overexpression in breast, pancreatic, and colon cancers (9, 11, 12). Interestingly, SgK269 exhibits a conserved molecular architecture and sequence similarity with a second pseudokinase, SgK223, the human ortholog of rat Pragmin (4, 13), suggesting that SgK269 and SgK223 are paralogs. SgK223 also exhibits a scaffolding function, regulating c-Src via recruitment of Csk to Tyr-411 (14) and associating with, and promoting activation of, Stat3 (15). As with SgK269, SgK223 is implicated in cancer. For example, Src-mediated SgK223 phosphorylation promotes cancer cell invasion (16). Furthermore, SgK223 is overexpressed in pancreatic cancer and enhances migration, invasion, and Stat3 activation in pancreatic ductal epithelial cells (15).

In this study we report, for the first time, direct interaction of the SgK269 and SgK223 pseudokinases, and we demonstrate that homo- and heterotypic association is a fundamental aspect of the signaling mechanism utilized by this small pseudokinase family. Given the scaffolding function of these proteins, we propose that the assembly of specific homo- or heterotypic complexes acts to determine signaling output, a novel regulatory mechanism among pseudokinases.

## Results

*Identification of SgK269 Domains Critical for Its Function in Mammary Epithelial Cells*—SgK269 and SgK223 exhibit a similar domain architecture (Fig. 1*a*), and the two proteins share significant sequence homology over the most N-terminal 100 amino acids, which exhibit a high $\alpha$-helical content, as well as the PK domain and a preceding short (43 amino acids) $\alpha$-helical segment, the latter designated as the CH region (Fig. 1*b*). This suggests that these proteins are paralogs, and the three homologous regions undertake critical conserved functions. Previously, we demonstrated that overexpression of SgK269 in MCF-10A-immortalized mammary epithelial cells perturbed cell phenotype and signaling in a manner consistent with SgK269 functioning as a breast cancer oncogene (11). To interrogate the function of specific regions of SgK269, we generated a series of deletion mutants lacking the N-terminal segment (ΔN), the CH region (ΔCH), and the pseudokinase domain (ΔPK) (Fig. 2*a*). Next, we stably overexpressed SgK269 and these mutants in MCF-10A-immortalized mammary epithelial cells (Fig. 2*b*). As reported previously (11), overexpression of full-length SgK269 (WT) resulted in cells displaying an elongated mesenchymal morphology (Fig. 2, *c* and *d*). Although this phenotype was also observed in cells expressing the ΔN mutant, cells expressing the ΔCH or ΔPK mutants displayed a wild-type morphology (Fig. 2, *c* and *d*). In addition, although overexpression of SgK269 was associated with decreased expression of E-cadherin and an increase in N-cadherin and vimentin levels, indicative of a partial epithelial-to-mesenchymal transition (11), these effects were compromised for all three deletion mutants (Fig. 2*b*). To determine the role of specific SgK269 regions in regulation of cell migration, we undertook wound-healing assays. Overexpression of WT SgK269 significantly enhanced cell migration compared with control cells (Fig. 2*e*), and although deletion of the N-terminal region had no discernable effect on activity in this assay, deletion of either the CH region or PK domain abolished the pro-migratory effect of SgK269 (Fig. 2*e*). Overall, these data indicate that whereas the role of the N-terminal region varies according to the biological end point analyzed, both the CH region and PK domain are critical for SgK269 function in this system.

*CH and PK Regions Are Implicated in Complex Formation between SgK269 and the Related Pseudokinase SgK223*—Given the known scaffolding role of SgK269 (9–11), we hypothesized that the CH and PK regions of SgK269 may mediate important protein-protein interactions. To identify SgK269 binding partners, we undertook LC-MS/MS analysis of anti-FLAG immunoprecipitates (IPs) prepared from MCF-10A cells expressing FLAG-tagged SgK269 (Fig. 3*a*). Proteins exhibiting significantly increased abundance in SgK269 IPs *versus* control IPs were identified (supplemental Dataset 1) and are presented in a volcano plot (Fig. 3*b*). Intriguingly, in addition to the known interactor Shc1 (10), these included SgK223. To confirm the interaction between SgK269 and SgK223, IP/Western blotting analyses were performed in MCF-10A cells stably overexpressing FLAG-tagged SgK269. Consistent with the MS data, endogenous SgK223 could be detected by Western blotting in SgK269 IPs (Fig. 4*a*). Additionally, co-immunoprecipitation of endogenous SgK269 and SgK223 could be demonstrated in both MCF-10A cells (Fig. 4*b*) and MDA-MB-231 breast cancer cells (Fig. 4*c*). To determine which regions of SgK269 mediate interaction with SgK223, we utilized the previously described deletion mutants (Fig. 1*a*). In addition, because SgK223 and SgK269 share close similarity in domain architecture (Fig. 4*d*), we generated a corresponding series of deletion mutants for SgK223. Co-immunoprecipitation with endogenous SgK223 could be readily demonstrated for WT and ΔN SgK269 but not for the ΔCH or ΔPK SgK269 mutants (Fig. 4*e*). Similarly, WT and ΔN SgK223 co-immunoprecipitated with endogenous SgK269, but this association was lost with the ΔCH or ΔPK SgK223 mutants

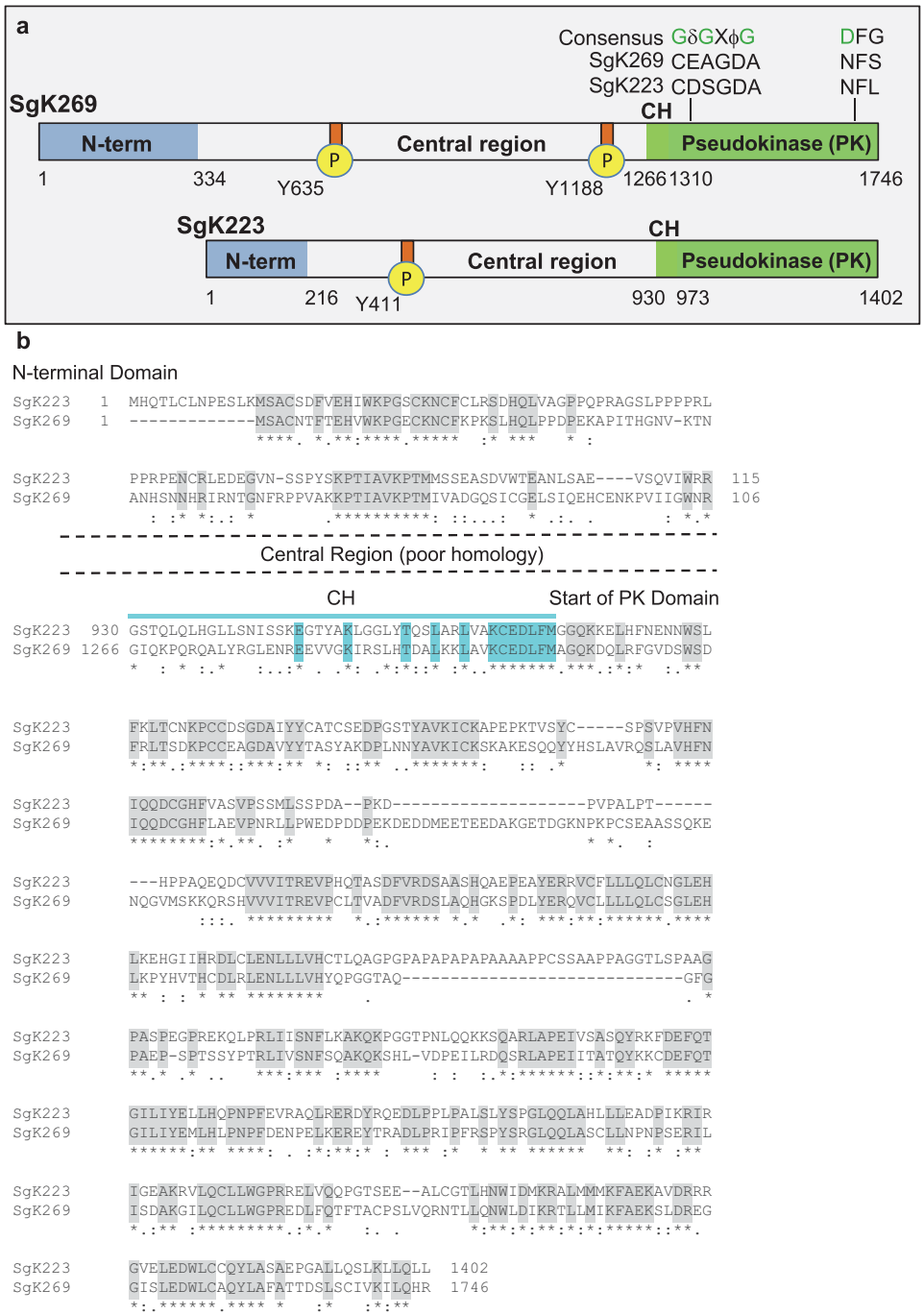


FIGURE 1. **SgK269 and SgK223 exhibit similar domain architecture and sequence homology.** *a,* schematic representation of SgK269 and SgK223. Substitutions in conserved residues important for protein kinase activity, as well as the location of key tyrosine phosphorylation sites, are *highlighted*. *b,* sequence alignment for the SgK269 and SgK223 proteins. The SgK269 and SgK223 proteins share marked sequence conservation (36%) in the first 106 residues of the N-terminal region and in the C-terminal 480 residues encompassing the CH region (*solid blue line*) and PK domain (51%). Amino acid identity in the CH region is *shaded blue*.

(Fig. 4*f*). These data implicate SgK223 in signaling by the SgK269 scaffold and indicate that the CH and PK regions of both SgK269 and SgK223 play a critical role in complex formation between these two proteins.

*SgK269 and SgK223 Undergo Homo- and Heterotypic Association*—Formation of dimers or higher order complexes between related signaling proteins is a commonly utilized mechanism to regulate and diversify signal output. Having demonstrated heterocomplex formation between SgK269 and SgK223, we tested whether these pseudokinases also self-associate. These experiments exploited a series of constructs for both SgK269 and SgK223 that involved HA-tagged WT proteins and FLAG/MYC-tagged WT and deletion mutants (Fig. 5*a*). Co-immunoprecipitation analysis from transfected HEK293T cells revealed that HA- and FLAG-tagged versions of WT SgK269 associated upon their co-expression, indicating that SgK269 forms homotypic complexes (Fig. 5*b*). However, this association was markedly reduced when the CH region was

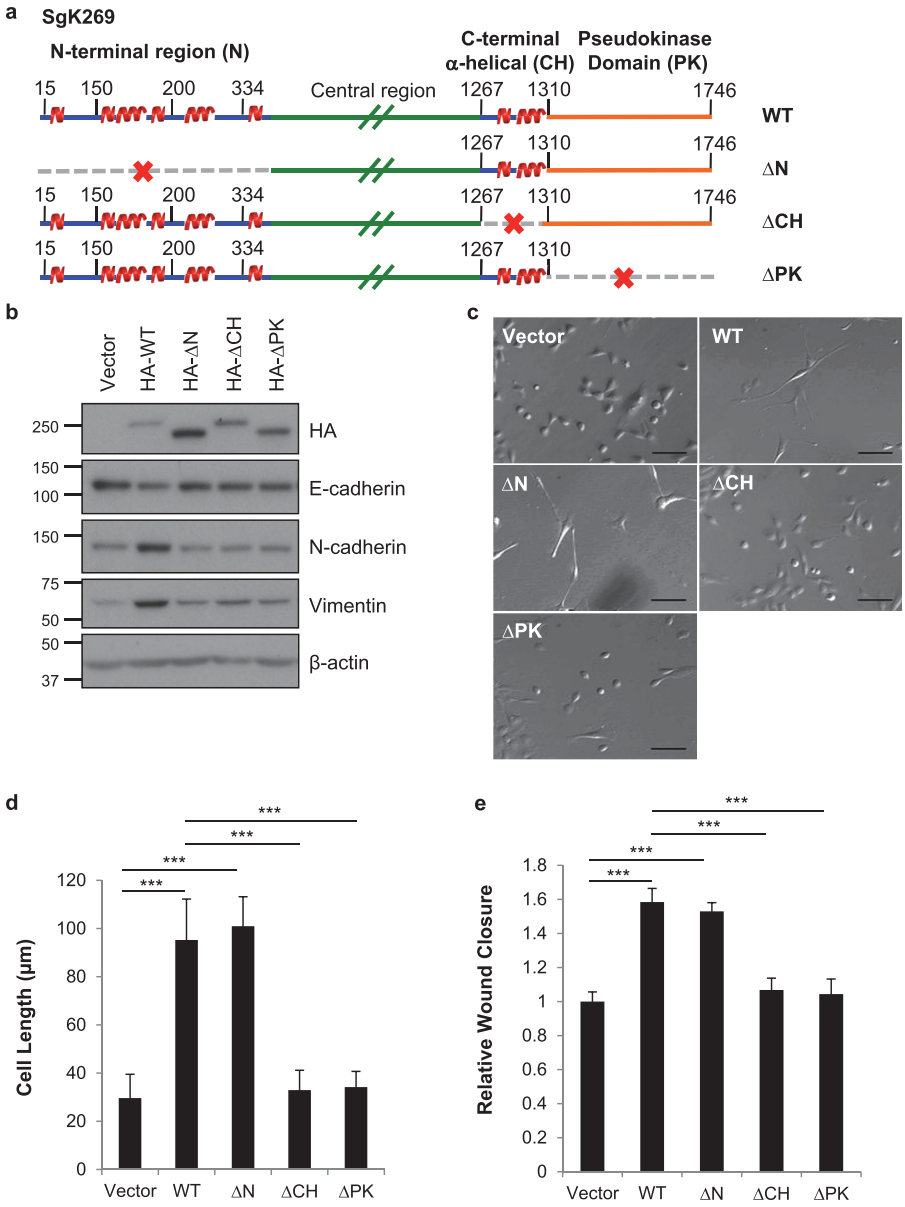


FIGURE 2. **Structure-function analysis of SgK269 identifies a key role for the CH and PK regions.** *a,* schematic representation of SgK269 and various truncation mutants (deleted regions indicated by a *red cross*), indicating secondary structure predictions for regions outside of the PK domain. The *central region* is predicted to be largely unstructured. *b,* expression of SgK269 wild type (*WT*) and different truncation mutants in MCF-10A cells. Western blotting for SgK269 (HA tag) and epithelial-to-mesenchymal transition markers was undertaken as indicated. Data are representative of three independent experiments. Positions of size markers (in kDa) are indicated. *c* and *d*, effects of overexpression of SgK269 and truncation mutants on cell morphology (*Scale bar,* 50 μm). The *histogram* indicates mean cell length for cell populations expressing SgK269 WT and the different mutants (mean ± S.E., ***, $p < 0.001$). *e,* effects of SgK269 and the mutants on cell migration. Relative wound closure was measured using ImageJ analysis software, and the results from three independent experiments are presented as a *histogram* (mean ± S.E., ***, $p < 0.001$). Data are expressed relative to the value for control cells (MCF-10A cells transfected with empty vector), which was arbitrarily set at 1.0.

deleted from one member of the complex and was almost abolished upon PK domain deletion (Fig. 5*b*). Self-association of SgK223 could also be demonstrated, and again, deletion of the CH region, and particularly the PK domain, reduced complex formation (Fig. 5*c*). These results demonstrate that the CH region and PK domain play significant roles in SgK269 and SgK223 homotypic association in cells.

To determine whether SgK269 and SgK223 directly interact, we utilized two approaches. First, we conducted pulldown assays. A GST fusion protein corresponding to the CH-PK region of SgK269 and immobilized on beads was able to pull down the corresponding region of SgK223 from solution, but not if the CH region was deleted from either the SgK269 or SgK223 partner protein (Fig. 6*a*). An equivalent result was obtained when this approach was applied to SgK269 or SgK223 homotypic interaction (Fig. 6, *b* and *c*), highlighting a key role for the CH region in direct homo- or heterotypic association of these pseudokinases. The second approach utilized was size-exclusion chromatography. Here, although a recombinant protein corresponding to the SgK223 PK domain was found to be mostly monomeric, the addition of the CH region resulted in a marked shift in the elution profile, indicative of the formation of higher molecular weight complexes (Fig. 7, *a* and *b*), consistent with the CH region mediating SgK223 homo-oligomerization.

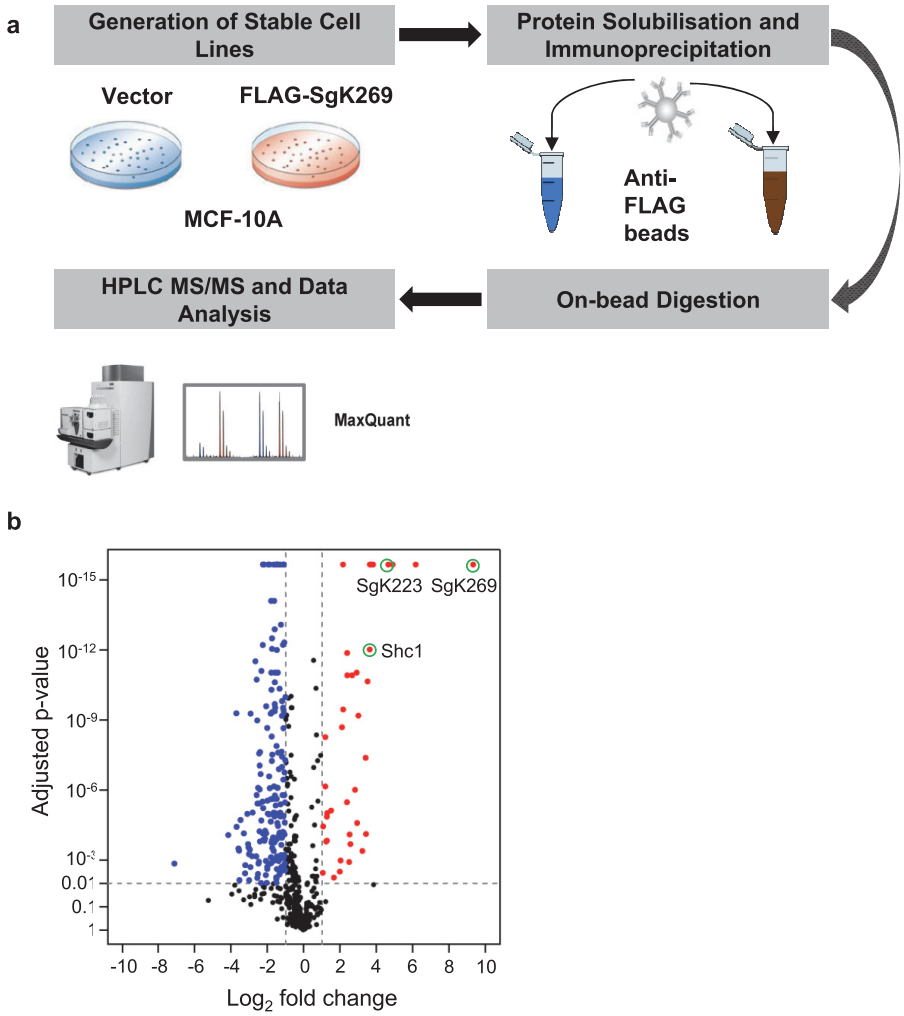


FIGURE 3. **Identification of novel SgK269 binding partners.** *a,* schematic of MS-based proteomics workflow. Anti-FLAG IPs prepared from MCF-10A cells expressing FLAG-tagged SgK269 were subjected to on-bead tryptic digestion. Resulting peptides were subjected to LC-MS/MS analysis. *b,* interactome of SgK269 represented as a *volcano plot* of the MS data. Proteins significantly enriched in the SgK269 IP with an adjusted *p* value ≤0.01 and a fold change of ≥2 against the control IP are displayed as *red dots*.

Deletion of the equivalent CH fragment in SgK269 resulted in a protein that still formed high molecular weight complexes, but with a broad elution profile indicative of mixed species (Fig. 7, *a* and *c*). These data suggest that the CH region in SgK269 may play an important role in controlling the stoichiometry of SgK269 oligomers.

To further characterize the role of the CH region in hetero-oligomerization, we conducted a range of size-exclusion experiments using various construct combinations. Pre-incubation of SgK269-CH-PK and SgK223-CH-PK prior to size-exclusion chromatography resulted in a marked shift in their elution profiles compared with when each protein was analyzed in isolation, suggestive of hetero-oligomerization (Fig. 7*d*). However, this shift was not observed when SgK269-CH-PK was pre-incubated with SgK223-PK (Fig. 7*e*). Overall, these data indicate that the SgK269 and SgK223 pseudokinases undergo homo- and heterotypic association, and they highlight a critical role for the CH region in this process. Also, because we readily see a shift to the higher molecular weight when mixing SgK223 and SgK269, and this shift is not seen when loading SgK223 and SgK269 alone at an equivalent concentration, it is likely that heterotypic interaction between SgK223 and SgK269 is more favorable than homotypic interaction of the individual proteins.

*Homo- and Heterotypic Association Regulates the Signaling Potential of SgK269 and SgK223*—The propensity for SgK269 and SgK223 to associate, coupled with their known scaffolding functions (10, 11, 14), led us to hypothesize that homo- *versus* heterotypic association of these pseudokinases may determine signal output and biological response and that heterotypic association represents a mechanism for signal diversification. If this hypothesis is correct, then assembly of a heterotypic complex should allow one pseudokinase to indirectly couple to a binding partner of the other. To test this model, we characterized association with Grb2, because SgK269 recruits this adaptor via Tyr-635 (11). In MDA-MB-231 breast cancer cells, both SgK269 and Grb2 could be readily detected in SgK223 IPs (Fig. 8). Similarly, both SgK269 and SgK223 co-immunoprecipitated with Grb2. However, siRNA-mediated knockdown of SgK269 markedly reduced association of SgK223 and Grb2, indicating that SgK269 bridges these two proteins (Fig. 8).

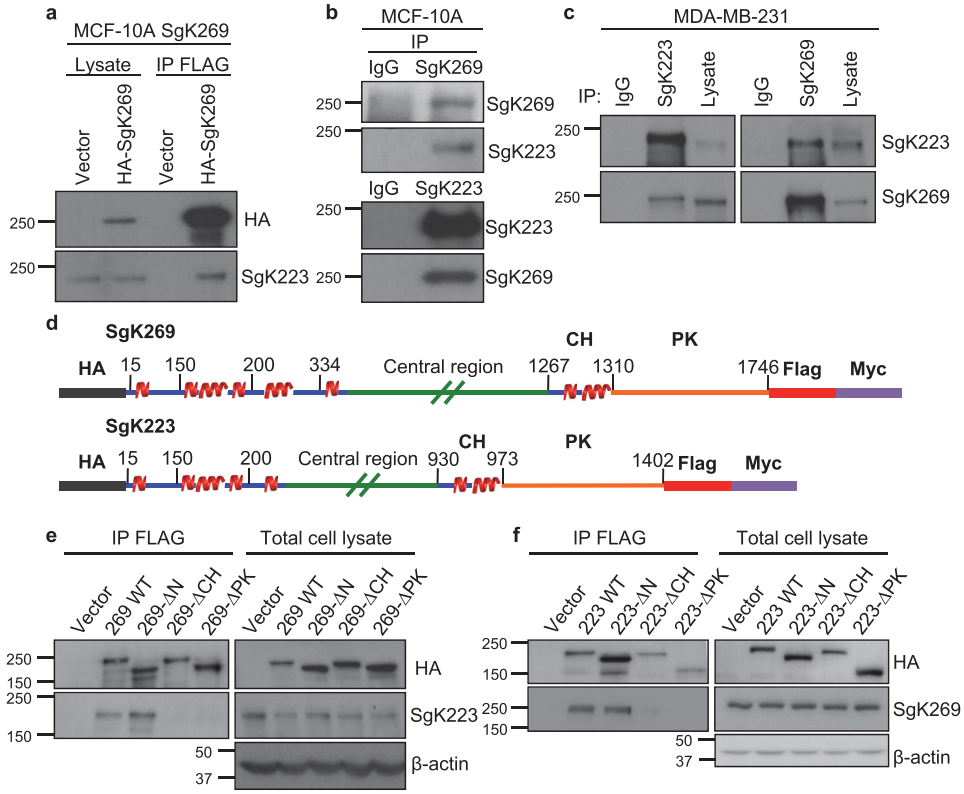


FIGURE 4. **CH and PK domains are critical for heterotypic association of SgK269 and SgK223.** *a–c,* SgK269 and SgK223 associate *in vivo*. Co-immunoprecipitation of exogenous FLAG/HA-tagged SgK269 with endogenous SgK223 in MCF-10A cells (*a*) and endogenous SgK269 and SgK223 in MCF-10A cells (*b*) and MDA-MB-231 breast cancer cells (*c*) is shown. IgG was used as a negative control for *b* and *c*. *d,* schematic representation of SgK269 and SgK223 wild-type constructs containing N-terminal HA tags and C-terminal FLAG and Myc tags. Truncation mutants were generated for both, which lacked the N-terminal region (Δ*N*), the C-terminal α-helical region (Δ*CH*), or the pseudokinase domain (Δ*PK*). *e* and *f,* identification of domains required for heterotypic association of SgK269 and SgK223. MCF-10A cells stably overexpressing epitope-tagged versions of the indicated SgK269 proteins (*e*) or SgK223 proteins (*f*) were harvested, and lysates were subjected to immunoprecipitation with an anti-FLAG antibody. IPs were blotted for HA and SgK223 (*e*) or SgK269 (*f*). All data are representative of at least two independent experiments.

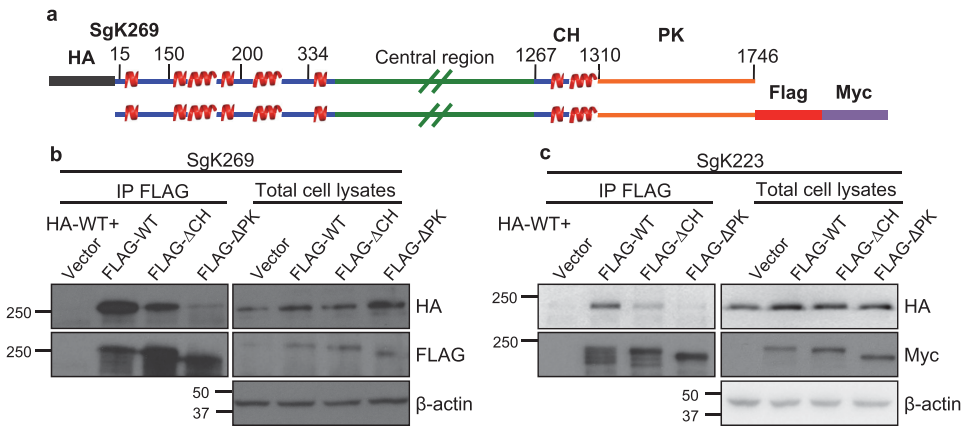


FIGURE 5. **CH and PK domains are critical for homotypic association of SgK269 and SgK223.** *a,* schematic representation of wild-type SgK269 with either HA tag or FLAG/Myc tags. Deletion mutants were generated with FLAG/Myc tags only. The same was undertaken for SgK223. *b* and *c,* identification of domains required for homotypic association of SgK269 and SgK223. HEK293 cells were co-transfected with plasmids encoding HA-tagged SgK269 (HA-WT) in combination with plasmids encoding FLAG/Myc-tagged SgK269 or different deletion mutants (*b*). Lysates were subject to immunoprecipitation with an anti-FLAG antibody and Western blotted anti-HA or anti-FLAG as indicated. *c,* same procedure was followed, but this time co-expressing HA-tagged SgK223 with FLAG/Myc-tagged SgK223 proteins. All data are representative of at least two independent experiments.

To further interrogate functional inter-relationships between the two pseudokinases, we determined how the presence of SgK223 influences SgK269 signaling potential. Two key biological end points of SgK269 overexpression in MCF-10A cells are increased cell migration and Stat3 activation (Fig. 1*e*) (11). Interestingly, overexpression of SgK223 in immortalized human pancreatic ductal epithelial cells also elicits these effects (15), raising the possibility that SgK269-mediated regulation of these end points involves SgK223. To test this hypothesis, we generated SgK223 knock-out (KO) MCF-10A cell lines using CRISPR/Cas9 and picked two clones for further studies (Fig. 9*a*). Wound healing assays demonstrated that the

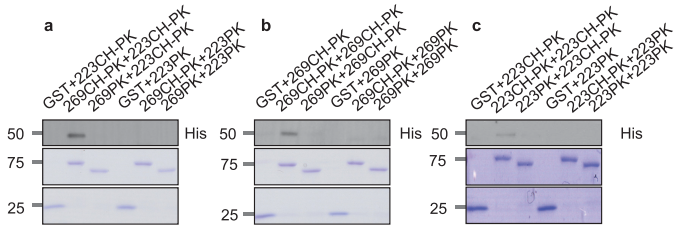


FIGURE 6. **CH region is critical for homotypic and heterotypic association of recombinant SgK269 and SgK223 C-terminal regions.** Equal amounts of SgK269 (*a* and *b*) or SgK223 (*c*) GST fusion proteins on beads were incubated with recombinant His-tagged SgK269 (*b*) or SgK223 (*a* and *c*) proteins, as indicated. Following washing, samples were analyzed either by Coomassie Blue staining (*bottom panels*) or by Western blotting with an anti-His tag antibody (*top panels*). GST was used as a negative control. *Numbers* on *left-hand side* of panels indicate position of corresponding size markers (sizes in kDa). All data are representative of at least two independent experiments.

migratory potential of MCF-10As was unaffected by SgK223 ablation (Fig. 9*b*). Next, we expressed WT SgK269 and SgK269 deletion mutants (Fig. 1*a*) in the SgK223 KO and parental MCF-10A cell lines at comparable levels (Fig. 9*c*). Comparison of the migratory potential of the resulting cell lines revealed that the ability of WT SgK269 to promote cell migration was significantly compromised in the absence of SgK223 (Fig. 9*d*). Given that the activity of SgK269 in this assay depends on the presence of the CH and PK domains (Fig. 1*e*), and both these regions are required for efficient SgK269/SgK223 interaction (Figs. 4, 6, and 7), this strongly suggests that optimal promotion of migration by SgK269 requires formation of SgK269-SgK223 heterocomplexes. However, in the absence of SgK223, WT and ΔN SgK269, but not the ΔCH and ΔPK mutants, still mediated a small but significant enhancement of migration, indicating that SgK269 homotypic complexes may also contribute to pro-migratory signaling (Fig. 9*e*).

Next, we sought to determine whether SgK269/SgK223 interaction is required for activation of the Stat3 signaling pathway in MCF-10A cells. Overexpression of WT or ΔN SgK269, but not the ΔCH or ΔPK mutants, in parental MCF-10A cells promoted Stat3 tyrosine phosphorylation on Tyr-705 (Fig. 10*a*), suggesting that SgK269 homo- or heterotypic association is required for this effect on downstream signaling. Interestingly, as observed for the human pancreatic ductal epithelial model (15), overexpression of SgK223 in MCF-10A cells enhanced Stat3 activation, and this was also dependent on the presence of the CH and PK domains (Fig. 10*b*). However, in the SgK223 KO cells, SgK269 failed to enhance Stat3 tyrosine phosphorylation (Fig. 10*c*). The domain dependence of this effect for both SgK269 and SgK223 in MCF-10A cells, coupled with the requirement for SgK223 in SgK269-mediated Stat3 phosphorylation, strongly implicates SgK269/SgK223 interaction in activation of this signaling pathway. To further test this model, we performed transient siRNA-mediated knockdown of SgK223 in SgK269-overexpressing MCF-10As. This resulted in a significant decrease in Stat3 tyrosine phosphorylation compared with the non-targeting control (Fig. 10*d*). We acknowledge the possibility of off-target effects mediated by the CRISPR/Cas9 approach, but the absence of an effect of SgK223 ablation on the baseline migration of MCF-10As, the reproducibility of the observed effects in two independent clones, and the similar effect of SgK223 knock-out and siRNA-mediated SgK223 knockdown on Stat3 regulation strongly support the validity of our conclusions. Overall, these data demonstrate that association of SgK269 with SgK223 is critical for the ability of SgK269 to enhance both cell migration and a critical oncogenic signaling pathway.

## Discussion

There is now strong evidence that pseudokinases can function as allosteric regulators and/or scaffolds. Thus, STRADα binds the *bona fide* protein kinase LKB1 as a pseudosubstrate and allosterically induces the kinase domain of LKB1 to adopt an active conformation, and ErbB3 transactivates ErbB1, -2, and -4 via kinase domain heterodimerization (3). ErbB3 is also a potent recruiter of phosphatidylinositol 3-kinase (PI3K), and dimerization with ErbB3 is a mechanism used by other ErbB receptors to activate the PI3K pathway and diversify their signal output (7). In the case of SgK269 and SgK223, identification of specific binding partners indicated a scaffolding function for these two pseudokinases (10, 11, 14). However, it was assumed that these two pseudokinases signal independently. In contrast, in this study, we demonstrate that SgK269 and SgK223 associate with each other and that heterocomplex formation bridges SgK223 to Grb2 and is required for the effects of SgK269 on cell migration and Stat3 activation. In addition, we report that these two proteins also form homotypic complexes. Given that the repertoire of known interactors differs for these two scaffolds, with SgK269 binding Grb2 and Shc1 (10, 11) and SgK223 recruiting Csk and Stat3 (14, 15), this leads to a model whereby homotypic *versus* heterotypic association of SgK223 and SgK269 acts as a novel mechanism to qualitatively and quantitatively regulate signal output over both space and time (Fig. 11*a*). Based on this model, a simple mechanism to modulate the proportion of homo- *versus* heterotypic complexes would be through altering the relative expression of the individual proteins, and supporting this concept, we note that certain breast cancer cell lines, such as MDA-MB-231, overexpress both SgK269 and SgK223 relative to MCF-10A cells, although BT-549 cells exhibit increased expression of only SgK269 (Fig. 11*b*).

In co-immunoprecipitation experiments from living cells, both the CH region and PK domain were required for optimal homo- and heterotypic association of SgK269 and SgK223. A key requirement for the CH region in homotypic or heterotypic association of SgK223 and SgK269 was confirmed by pulldown assays using recombinant proteins. Upon size-exclusion chromatography, undertaken at higher protein concentrations and different buffer conditions to pulldowns, deletion of the CH region from CH-PK proteins led to a reduced formation of dimer in the case of SgK223, but it did not affect the ability of SgK269 to multimerize. However, the SgK269 PK domain had the propensity to form a range of multimeric species as indicated by a broader elution profile compared with CH-PK SgK269. In addition, removal of this region from SgK223 CH-PK prevented heterotypic association with SgK269 CH-PK. Together, the *in vitro* and *in vivo* data suggest that both the CH and PK region contribute to the formation of a stable complex between SgK223 and SgK269, and both might be necessary to maintain ordered oligomers. In terms of stoichiome-

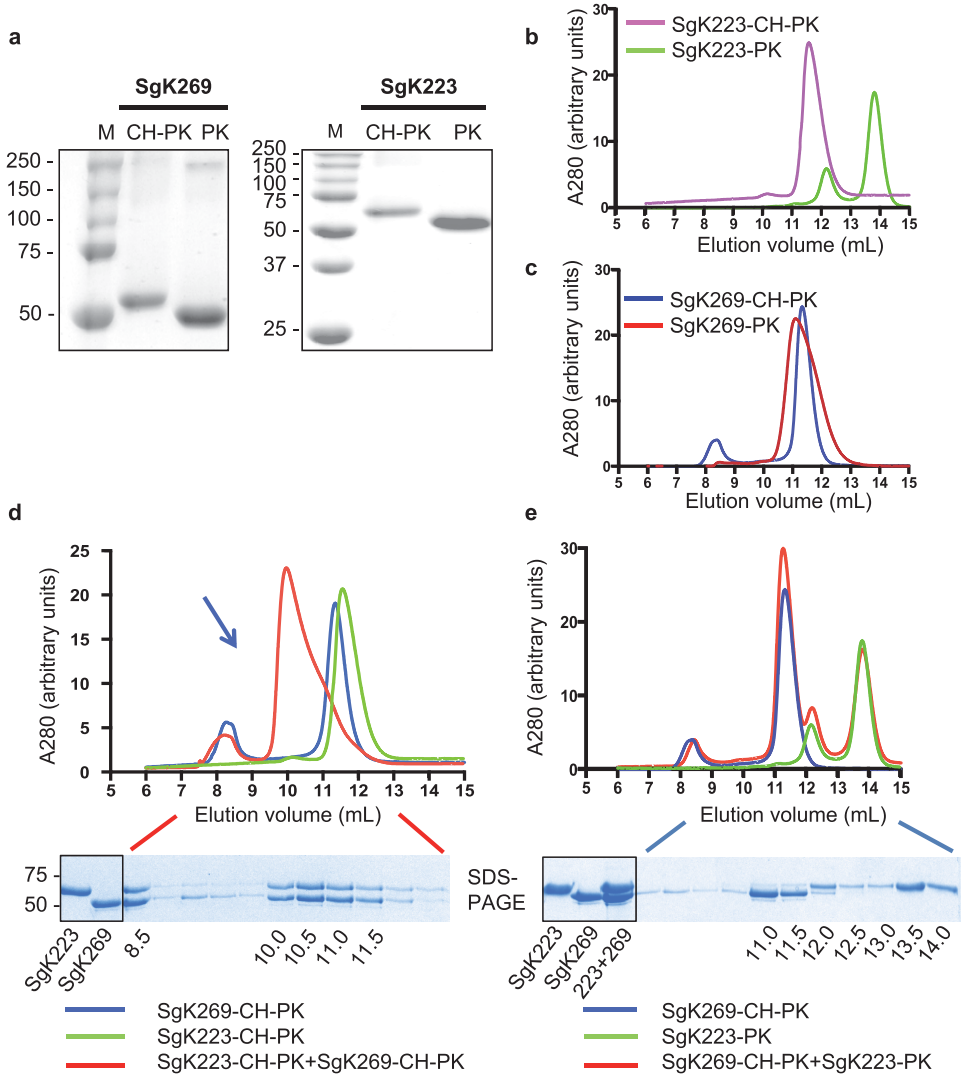


FIGURE 7. **Characterization of homotypic and heterotypic association of recombinant SgK269 and SgK223 C-terminal regions via size-exclusion chromatography.** *a,* Coomassie staining of purified recombinant His-tagged SgK269 and SgK223 CH-PK and PK proteins used for size-exclusion chromatography. *b* and *c,* size-exclusion chromatography. Elution profile of SgK223-CH-PK was compared with SgK223-PK (*b*). Elution profile of SgK269-CH-PK was compared with SgK269-PK (*c*). Elution profiles of SgK269-CH-PK + SgK223-CH-PK (*d*) and SgK269-CH-PK + SgK223-PK (*e*) were compared with their individual elution profiles. The *arrow* highlights the shift in elution profile upon complex formation. Also shown are corresponding Coomassie-stained gel fractions highlighting complex formation (*d*) and its absence (*e*). All data are representative of at least three independent experiments.

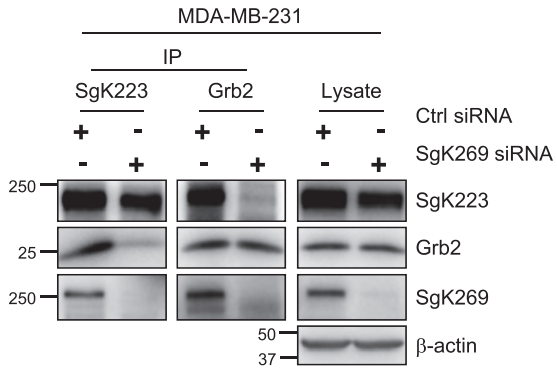


FIGURE 8. **Association of SgK223 with Grb2 is dependent on SgK269.** MDA-MB-231 cells were subject to siRNA-mediated knockdown of SgK269. SgK223 and Grb2 IPs and cell lysates from control and SgK269 knockdown cells were subject to Western blotting as indicated. Data are representative of two independent experiments.

try, SDS-PAGE analysis of the complex formed between SgK269 and SgK223 CH-PK proteins strongly indicate a one to one ratio (Fig. 6), but further biophysical studies are required to determine the exact stoichiometry of the complex, *i.e.* whether the complex is driven by dimer-dimer interactions between SgK269 and SgK223. The identification of the primary interaction interface(s) for homotypic and heterotypic association will provide critical insights into the nature of these complexes and the underlying mechanism for their assembly.

The demonstrated homotypic and heterotypic association of SgK269 and SgK223 raises interesting questions regarding potential interactions between the juxtapositioned pseudokinase domains, and what roles these may play. Although the pseudokinase domains of ErbB3 and STRAD$\alpha$ are known to function as direct allosteric activators of *bona fide* kinases, neither SgK269 nor SgK223 possesses nucleotide binding activity

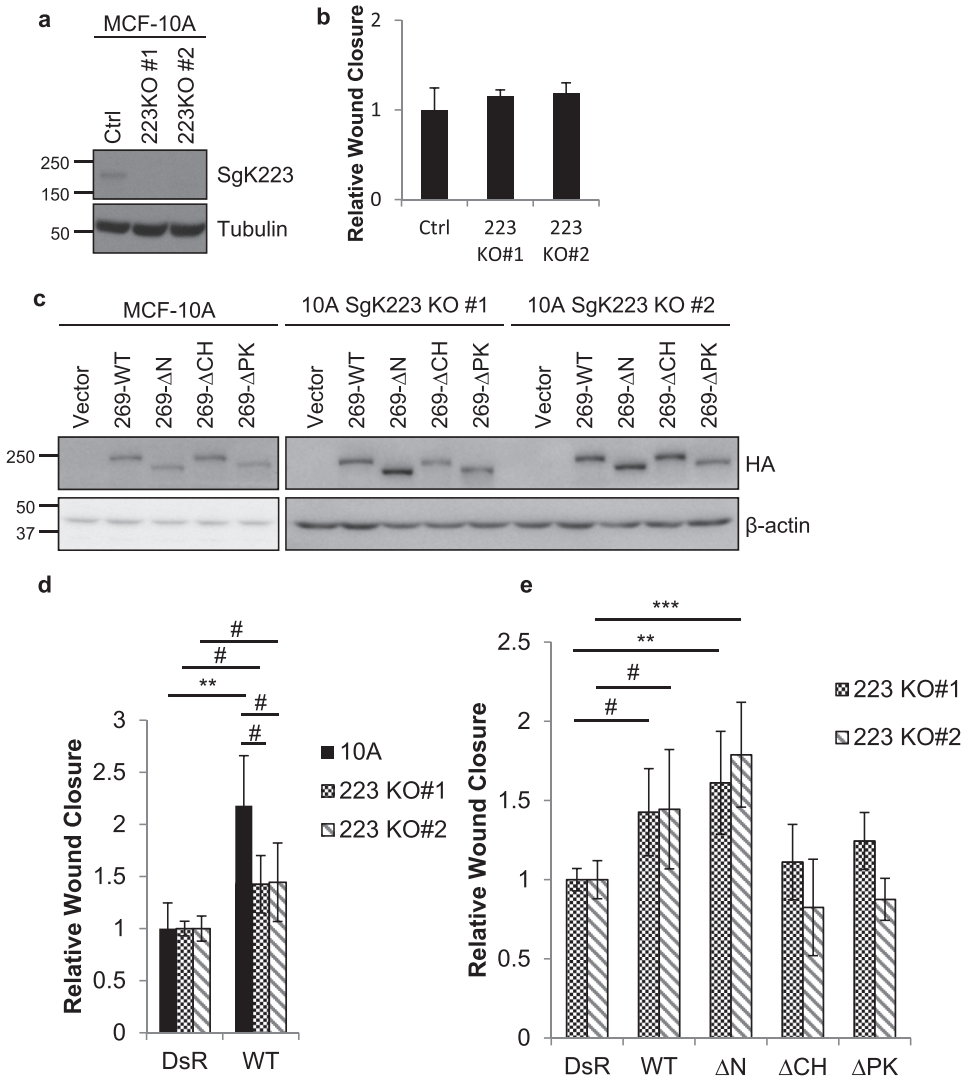


FIGURE 9. **Regulation of pseudokinase signal output by homo- and heterotypic association.** *a,* characterization of SgK223 knock-out (*KO*) MCF-10A cells generated by CRISPR/Cas9. Western blotting was undertaken as indicated. *b,* relative migration rates of control (*Ctrl*) MCF-10A and SgK223 KO cells. Relative wound closure was measured using ImageJ analysis software, and results from three independent experiments are presented as a histogram. Data are expressed relative to the value for MCF-10A cells, which was arbitrarily set at 1.0. *c,* expression of SgK269 WT and deletion mutants in MCF-10A and SgK223 KO cells. Western blotting was undertaken as indicated. *d,* effect of SgK269 on cell migration in MCF-10A and SgK223 KO cells. Relative wound closure was assessed as in *b* and is expressed relative to cells transfected with empty vector (*DsR*), which was arbitrarily set at 1.0. Data represent mean ± S.E., **, $p < 0.01$; #, $p < 0.05$. *e,* effect of SgK269 WT and deletion mutants on cell migration in SgK223 KO cells. Data represent mean ± S.E., **, $p < 0.01$; ***, $p < 0.001$; #, $p < 0.05$.

(4), indicating that interaction cannot mediate trans-regulation of phosphotransferase activity of one or both proteins. Given the known scaffolding role of these pseudokinases, one possibility is that association of the SgK223 and SgK269 PK domains is used as a mechanism to generate a specific interface for protein/protein interactions with effector proteins, which may differ between homotypic and heterotypic complexes (Fig. 11).

Previously, we reported that overexpression of either SgK269 or SgK223 promoted cell migration and Stat3 activation (11, 15). A simple interpretation of these data is that they reflect conserved functions for two related pseudokinases. However, we now report that SgK269 and SgK223 exhibit an intimate functional as well as physical relationship, with their combined signal output dependent on the ability to form higher heteromeric complexes. Use of SgK223-deficient MCF-10A cells demonstrated that Stat3 activation, and maximal promotion of migration, by SgK269 is dependent on the presence of SgK223. This likely reflects, at least in part, the demonstrated ability of SgK223 to associate with Stat3 (15) and indicates that the two pseudokinases utilize a trans-regulatory mechanism for triggering specific signaling pathways, reminiscent of that engaged by members of the ErbB family of kinases. Given that SgK223 binds Csk and sequesters it away from the plasma membrane, leading to Src activation (14), and that SgK269 is also known to positively regulate Src (12), it is possible that interaction of these two pseudokinases also acts as a novel mechanism to regulate Src activity in a spatial manner. Overall, our data identify a novel signaling mechanism for pseudokinases that may function to regulate several important signal transduction pathways, and we demonstrate that homo- and heterotypic assembly of scaffolding proteins with contrasting complements of SH2 and PTB domain binding sites is not the sole property of *bona fide* kinases such as members of the ErbB family.

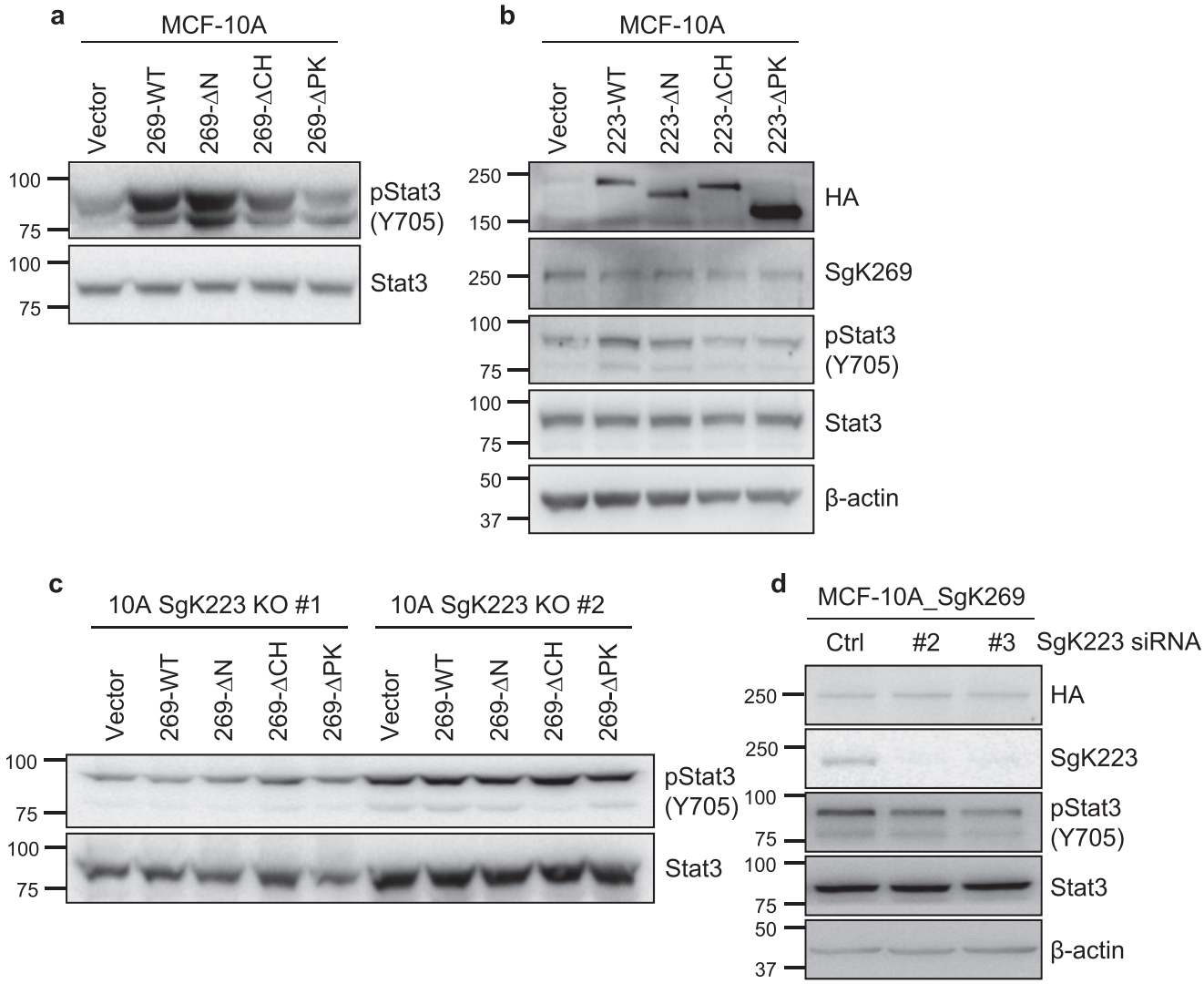


FIGURE 10. **Enhancement of Stat3 activation by SgK269 requires SgK223.** *a* and *b,* SgK269 and SgK223 promote Stat3 activation in MCF-10A cells in a CH and PK domain-dependent manner. Lysates from MCF-10A cells expressing SgK269 (*a*) or SgK223 (*b*) WT or deletion mutants were subject to Western blotting analysis as indicated. *c,* SgK269 fails to enhance Stat3 activation in SgK223 KO MCF-10A cells. The panels show Western blotting of lysates prepared from two individual SgK223 KO cell lines expressing SgK269 WT or deletion mutants. *d,* knockdown of SgK223 in SgK269-overexpressing MCF-10A cells reduces Stat3 tyrosine phosphorylation. Lysates from cells transfected with control siRNA or two independent SgK223-selective siRNAs were Western blotted as shown. All data representative of at least two independent experiments.

## Experimental Procedures

*Plasmids*—The retroviral expression vector pRetroX-IRES containing N-terminal HA-tagged and C-terminal FLAG/Myc-tagged SgK269 was previously generated in our laboratory (11). A codon-optimized cDNA encoding N-terminal HA-tagged and C-terminal FLAG-tagged SgK223 was synthesized by Genscript and cloned into the BglII and EcoRI restriction sites of the pMIG-Sapphire Express vector. Generation of deletion mutants ΔN, ΔCH, and ΔPK, and addition of different tags, was achieved via PCR using the primers listed in supplemental Table S1 and subcloning into pRetroX-IRES (SgK269 constructs) and pMIG-Sapphire Express (SgK223 constructs).

For generation of GST fusion proteins for pulldown assays, DNA fragments encoding SgK269/SgK223 CH-PK or PK regions were subcloned into pGEX-4T-1 (GE Healthcare, Little Chalfont, Buckinghamshire, UK). Protein boundaries were as follows: hSgK223-CH-PK(930–1402), hSgK223-PK(973–1402), hSgK269-CH-PK(1267–1746), and hSgK269-PK(1310–1746). For interaction studies using size-exclusion chromatography, the same DNA fragments were subcloned into pCOLD IV (Takara) and modified to incorporate an N-terminal tobacco etch virus-cleavable $His_6$ tag.

*Antibodies*—Antibodies against E-cadherin (catalog no. 3195P), N-cadherin (catalog no. 13116P), vimentin (catalog no. 5741S), Myc (catalog no. 2276), GST (catalog no. 2625P), Grb2 (catalog no. 3972S), tubulin (catalog no. 2125S), pStat3 Y705 (catalog no. 9138S), and Stat3 (catalog no. 9139S) were purchased from Cell Signaling Technology (Danvers, MA). β-Actin (catalog no. sc-69879), normal rabbit IgG (catalog no. sc-2027), normal mouse IgG (catalog no. sc-2025), and SgK269 antibodies (catalog no. sc-100403) were purchased from Santa Cruz Biotechnology (Dallas, TX); HA (catalog. 11867423001) was purchased from Roche Applied Science (Mannheim, Ger-

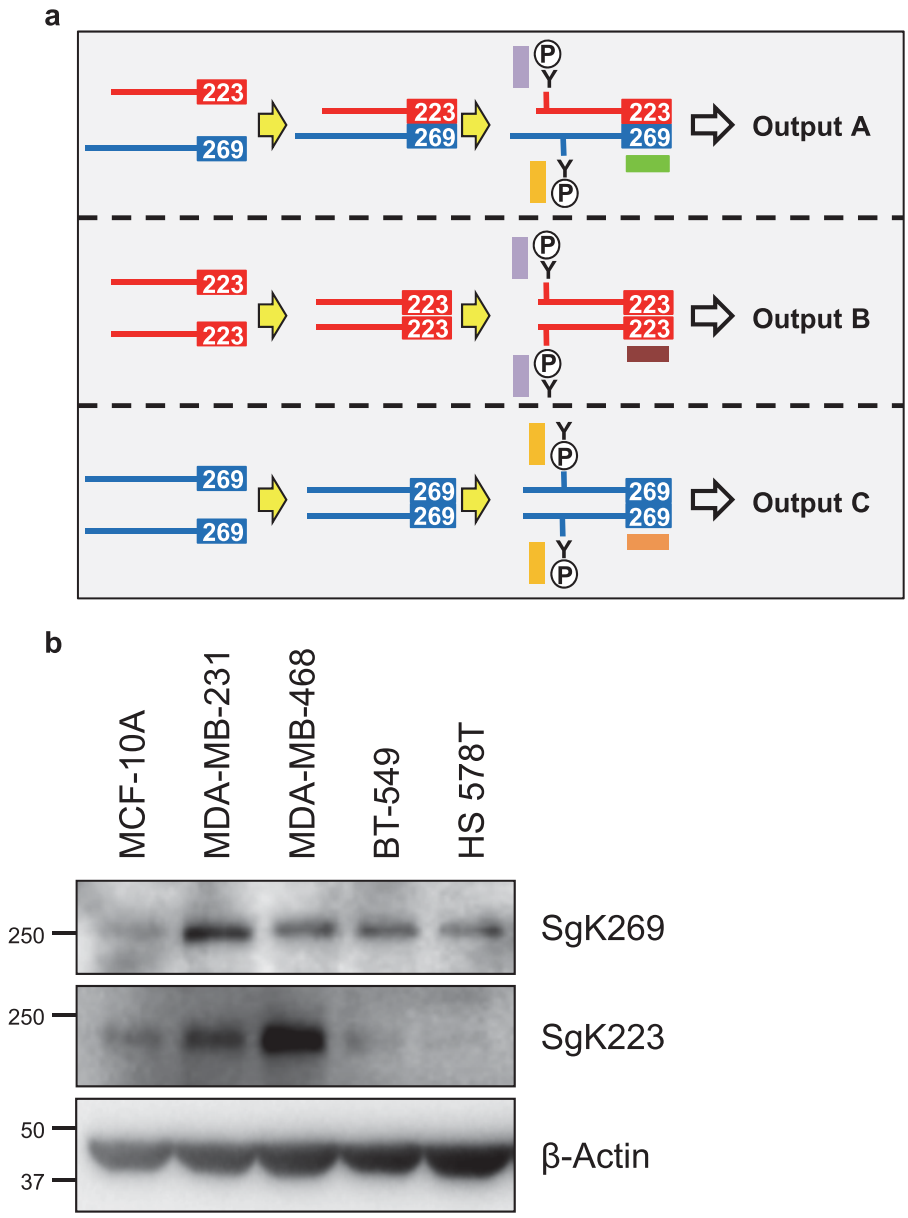


FIGURE 11. **Homo- and heterotypic association of the SgK269 and SgK223 pseudokinase scaffolds as a mechanism to regulate signal output.** *a,* proposed model. SgK269 and SgK223 recruit distinct repertoires of SH2 or PTB domain-containing signaling proteins to their contrasting complement of tyrosine phosphorylation sites. Reflecting this, homotypic and heterotypic complexes generate contrasting integrated signals. In this model, we have also proposed that the PK domains provide a selective binding interface upon interaction that differs between homotypic and heterotypic complexes. *b,* differential expression of SgK269 and SgK223 among breast epithelial and breast cancer cell lines, as detected by Western blotting.

many); His (catalog no. 552565) was from BD Pharmingen, and FLAG (catalog no. F1804) from Sigma. The SgK223 antibody was custom-made (15).

*Tissue Culture and Generation of Stable Cell Lines*—MCF-10A cells stably expressing the murine ecotropic receptor (MCF-10A ecotropic receptor) were maintained as reported previously (17). Breast cancer cell lines were sourced and maintained as described previously (11). The packaging cell line PlatE was used for retrovirus production, and MCF-10A cells were infected with retrovirus as detailed previously (18). The CRISPR/Cas9 approach was used for generation of SgK223 knock-out (KO) lines in MCF-10A cells. The single guide RNAs targeting SgK223 exon 2 was designed using the CRISPR DESIGN tool (supplemental Table S1).

The single guide RNAs were annealed and subcloned into the pSpCas9(BB) construct described by Ran *et al.* (19). MCF-10A ecotropic receptor cells were transiently transfected with the resulting constructs using Lipofectamine 3000 according to the manufacturer's instructions. FACS was used to isolate GFP-positive cells that were individually seeded into separate wells of a 96-well plate. Cells were expanded and screened for the absence of SgK223 using PCR and immunoblotting.

*Cell Lysis, Immunoprecipitation, and Immunoblotting*—Cell lysates for immunoblotting and co-immunoprecipitation were prepared using RIPA and normal lysis buffers, respectively (17). For co-immunoprecipitation, cell lysates were incubated with either primary antibody conjugated to protein G beads or anti-FLAG M2 affinity-agarose beads (Sigma) at 4 °C overnight on a

shaking platform. Following extensive washing with ice-cold lysis buffer, the immune complexes were eluted with SDS-PAGE loading buffer and subjected to Western blotting analysis.

*Wound Healing Assay*—MCF-10A cells were seeded in 24-well plates at $2.5 \times 10^5$ cells/well in triplicate. Wounds were made by scraping with a 200-$\mu$l plastic pipette tip across the cell monolayer, and then the cells were cultured with 5 $\mu$g/ml mitomycin C to prevent cell division. Phase contrast images were recorded at 0 and 20 h using an EVOS f1 (Advanced Microscopy Group, Bothell, WA). Wound areas were subsequently quantified using ImageJ software (version 10.2).

*Recombinant Protein Expression and Purification*—Recombinant His-tagged proteins were expressed in *Escherichia coli* C41(DE3) cells cultured in 2YT medium at 37 °C and induced with 0.2 mM isopropyl 1-thio-$\beta$-D-galactopyranoside at 16 °C overnight. For the SgK223 constructs, cells were harvested and resuspended in lysis buffer comprising 20 mM Tris, pH 8.5, 500 mM NaCl, 10% glycerol, 5 mM imidazole, 0.1% Thesit, 5 mM DTT. Following sonication, the supernatant was clarified by centrifugation (for 30 min at 4 °C), and the proteins were purified by nickel affinity (Roche Applied Science) followed by a size-exclusion chromatography (Superdex-200 16/60, GE Healthcare) in 20 mM Tris, pH 8.5, 200 mM NaCl, 1 mM TCEP. The pure protein fractions were concentrated and stored in storage buffer (20 mM Tris, pH 8.5, 200 mM NaCl, 5% glycerol, 1 mM TCEP) at −80 °C. The same methodology was followed for the purification of SgK269 constructs except that the pH of all buffers was changed to 7.5.

The pGEX vectors encoding various GST-tagged SgK269 and SgK223 CH-PK/PK proteins were expressed in BL21 cells cultured in 2YT media containing 100 $\mu$g/ml ampicillin at 37 °C and induced with 0.2 mM isopropyl 1-thio-$\beta$-D-galactopyranoside for 4 h. The bacterial pellet was resuspended in 20 ml of 1× PBS containing 0.5 mM dithiothreitol (DTT) and 1% Triton X-100 and lysed by sonication. The supernatant was clarified by centrifugation at 12,000 × *g* for 30 min at 4 °C and loaded onto glutathione-Sepharose 4B beads (GE Healthcare). After extensive washes with washing buffer (1× PBS, 0.5 mM DTT, 1% Triton X-100), the GST fusion proteins were eluted with 50 mM Tris, pH 8.0, 200 mM NaCl, 5 mM DTT, 10 mM glutathione. Fractions containing the GST fusions protein were then loaded onto a size-exclusion chromatography column (Superdex-200 16/60, GE Healthcare) using 20 mM Tris, pH 7.5, 200 mM NaCl, 1 mM TCEP, concentrated, and stored in the same buffer.

*GST Pulldown Assay*—GST-tagged proteins bound to glutathione-Sepharose 4B beads were incubated with His-tagged proteins for 2 h at 4 °C on a rotating platform. The pulldowns utilized 1 $\mu$g of GST-tagged protein in 200 $\mu$l of lysis buffer (30 mM Tris, 300 mM NaCl, 1 mM TCEP, pH 7.5) containing 1 $\mu$g of His-tagged protein. The beads were recovered by centrifugation (500 × *g*, 15 s, 4 °C), washed three times with lysis buffer, resuspended in SDS-PAGE loading buffer, and then subjected to Western blotting analysis.

*Interaction Studies Using Size-exclusion Chromatography*—For complex formation studies, 50 $\mu$l of purified SgK223-CH-PK (or SgK223-PK) at 60 $\mu$M was incubated with 50 $\mu$l of purified SgK269-CH-PK at 80 $\mu$M to achieve a 1:1.3 ratio and loaded onto an S200 10/300 GL column with a flow rate of 0.5 ml/min in 20 mM Tris, pH 8.5, 200 mM NaCl, 5% glycerol, 1 mM TCEP. Control runs were performed by running 50 $\mu$l of each individual protein, SgK223-CH-PK, SgK223-PK, SgK269-CH-PK, and SgK269-PK, in the same buffer. The same elution profiles were obtained in three independent experiments.

*siRNA Treatment*—The Universal Negative Control #1 (SIC001) and the SgK223-selective siRNAs (SASI_Hs02_0031603-4 and -5) used were obtained from Sigma, and siRNA was applied to cells using DharmaFECT 3 (Dharmacon, Lafayette, CO) transfection reagent according to the manufacturer's instructions. Cells were lysed 72 h post-transfection using RIPA buffer. The siRNA negative control, ON-TARGETplus Non-targeting Pool, and the ON-TARGETplus set of four SgK269/PEAK1 siRNAs (LU-005339-00-0010) were obtained from Dharmacon, and siRNA was applied to cells using DharmaFECT 4 (Dharmacon) transfection reagent according to the manufacturer's instructions. Cells were lysed 72 h post-transfection using normal lysis buffer.

*Identification of SgK269 Binding Partners by MS-based Proteomics*—Control MCF-10A cells or cells expressing FLAG/HA-tagged SgK269 were lysed in normal lysis buffer (17). Cell lysate (2 mg) was precleared using recombinant protein G-Sepharose 4B beads (Invitrogen) and then incubated with 10 $\mu$l of anti-FLAG M2 affinity beads (Sigma) overnight at 4 °C. Following washing with lysis buffer and then ammonium bicarbonate buffer, the immunocomplex was subjected to on-bead digestion with trypsin, and the resulting peptides were analyzed by LC-MS/MS on a Thermo Scientific (Waltham, MA) Q-Exactive MS instrument. Peptides were separated by nano-LC using an UltiMate 3000 high performance liquid chromatography and autosampler system (Dionex, Sunnyvale, CA). Samples were subjected to positive nanoflow electrospray analysis in information-dependent acquisition mode (250 nl/min for 30 min). Raw files were processed with MaxQuant (20) (version 1.5.2.8). We used the MaxLFQ algorithm for label-free quantification (21), including the "match between runs" option. MSstasts (version 2.0) (22) was used to normalize the data, impute for missing values, compute fold changes, and used for significance testing, including a *p* value correction by the Benjamini-Hochberg method (23). Candidate interacting proteins were defined by applying the following criteria: adjusted *p* value ≤0.01 with a fold change of ≥2 against the control IP. The mass spectrometry proteomics data have been deposited to the ProteomeXchange Consortium via the PRIDE (24) partner repository with the dataset identifier PXD004250.

*Author Contributions*—L. L., Y. W. P., R. S. L., X. M., Y. J., E. S. H., H. C., R. S., P. C. O., W. D., and I. S. L. provided experimental data. D. N. S. assisted with experimental design, and K. N. undertook MS data analysis. I. S. L. and R. J. D. wrote the manuscript with input from L. L. and coordinated the study.

**References**

1. Manning, G., Whyte, D. B., Martinez, R., Hunter, T., and Sudarsanam, S. (2002) The protein kinase complement of the human genome. *Science* **298,** 1912–1934

2. Reiterer, V., Eyers, P. A., and Farhan, H. (2014) Day of the dead: pseudokinases and pseudophosphatases in physiology and disease. *Trends Cell Biol.* **24,** 489–505
3. Zeqiraj, E., and van Aalten, D. M. (2010) Pseudokinases–remnants of evolution or key allosteric regulators? *Curr. Opin. Struct. Biol.* **20,** 772–781
4. Murphy, J. M., Zhang, Q., Young, S. N., Reese, M. L., Bailey, F. P., Eyers, P. A., Ungureanu, D., Hammaren, H., Silvennoinen, O., Varghese, L. N., Chen, K., Tripaydonis, A., Jura, N., Fukuda, K., Qin, J., *et al.* (2014) A robust methodology to subclassify pseudokinases based on their nucleotide-binding properties. *Biochem. J.* **457,** 323–334
5. Kovacs, E., Zorn, J. A., Huang, Y., Barros, T., and Kuriyan, J. (2015) A structural perspective on the regulation of the epidermal growth factor receptor. *Annu. Rev. Biochem.* **84,** 739–764
6. Lavoie, H., Li, J. J., Thevakumaran, N., Therrien, M., and Sicheri, F. (2014) Dimerization-induced allostery in protein kinase regulation. *Trends Biochem. Sci.* **39,** 475–486
7. Citri, A., and Yarden, Y. (2006) EGF-ERBB Signaling: towards the systems level. *Nat. Rev. Mol. Cell Biol.* **7,** 505–516
8. Christie, M., Boland, A., Huntzinger, E., Weichenrieder, O., and Izaurralde, E. (2013) Structure of the PAN3 pseudokinase reveals the basis for interactions with the PAN2 deadenylase and the GW182 proteins. *Mol. Cell* **51,** 360–373
9. Wang, Y., Kelber, J. A., Tran Cao, H. S., Cantin, G. T., Lin, R., Wang, W., Kaushal, S., Bristow, J. M., Edgington, T. S., Hoffman, R. M., Bouvet, M., Yates, J. R., 3rd, and Klemke, R. L. (2010) Pseudopodium-enriched atypical kinase 1 regulates the cytoskeleton and cancer progression [corrected]. *Proc. Natl. Acad. Sci. U.S.A.* **107,** 10920–10925
10. Zheng, Y., Zhang, C., Croucher, D. R., Soliman, M. A., St-Denis, N., Pasculescu, A., Taylor, L., Tate, S. A., Hardy, W. R., Colwill, K., Dai, A. Y., Bagshaw, R., Dennis, J. W., Gingras, A. C., Daly, R. J., and Pawson, T. (2013) Temporal regulation of EGF signaling networks by the scaffold protein Shc1. *Nature* **499,** 166–171
11. Croucher, D. R., Hochgräfe, F., Zhang, L., Liu, L., Lyons, R. J., Rickwood, D., Tactacan, C. M., Browne, B. C., Ali, N., Chan, H., Shearer, R., Gallego-Ortega, D., Saunders, D. N., Swarbrick, A., and Daly, R. J. (2013) Involvement of Lyn and the atypical kinase SgK269/PEAK1 in a basal breast cancer signaling pathway. *Cancer Res.* **73,** 1969–1980
12. Kelber, J. A., Reno, T., Kaushal, S., Metildi, C., Wright, T., Stoletov, K., Weems, J. M., Park, F. D., Mose, E., Wang, Y., Hoffman, R. M., Lowy, A. M., Bouvet, M., and Klemke, R. L. (2012) KRas induces a Src/PEAK1/ErbB2 kinase amplification loop that drives metastatic growth and therapy resistance in pancreatic cancer. *Cancer Res.* **72,** 2554–2564
13. Tanaka, H., Katoh, H., and Negishi, M. (2006) Pragmin, a novel effector of Rnd2 GTPase, stimulates RhoA activity. *J. Biol. Chem.* **281,** 10355–10364
14. Safari, F., Murata-Kamiya, N., Saito, Y., and Hatakeyama, M. (2011) Mammalian Pragmin regulates Src family kinases via the Glu-Pro-Ile-Tyr-Ala (EPIYA) motif that is exploited by bacterial effectors. *Proc. Natl. Acad. Sci. U.S.A.* **108,** 14938–14943
15. Tactacan, C. M., Phua, Y. W., Liu, L., Zhang, L., Humphrey, E. S., Cowley, M., Pinese, M., Biankin, A. V., and Daly, R. J. (2015) The pseudokinase SgK223 promotes invasion of pancreatic ductal epithelial cells through JAK1/Stat3 signaling. *Mol. Cancer* **14,** 139
16. Leroy, C., Fialin, C., Sirvent, A., Simon, V., Urbach, S., Poncet, J., Robert, B., Jouin, P., and Roche, S. (2009) Quantitative phosphoproteomics reveals a cluster of tyrosine kinases that mediates SRC invasive activity in advanced colon carcinoma cells. *Cancer Res.* **69,** 2279–2286
17. Brummer, T., Schramek, D., Hayes, V. M., Bennett, H. L., Caldon, C. E., Musgrove, E. A., and Daly, R. J. (2006) Increased proliferation and altered growth factor dependence of human mammary epithelial cells overexpressing the Gab2 docking protein. *J. Biol. Chem.* **281,** 626–637
18. Croucher, D. R., Rickwood, D., Tactacan, C. M., Musgrove, E. A., and Daly, R. J. (2010) Cortactin modulates RhoA activation and expression of Cip/Kip cyclin-dependent kinase inhibitors to promote cell cycle progression in 11q13-amplified head and neck squamous cell carcinoma cells. *Mol. Cell. Biol.* **30,** 5057–5070
19. Ran, F. A., Hsu, P. D., Wright, J., Agarwala, V., Scott, D. A., and Zhang, F. (2013) Genome engineering using the CRISPR-Cas9 system. *Nat. Protoc.* **8,** 2281–2308
20. Cox, J., and Mann, M. (2008) MaxQuant enables high peptide identification rates, individualized p.p.b.-range mass accuracies and proteome-wide protein quantification. *Nat. Biotechnol.* **26,** 1367–1372
21. Cox, J., Hein, M. Y., Luber, C. A., Paron, I., Nagaraj, N., and Mann, M. (2014) Accurate proteome-wide label-free quantification by delayed normalization and maximal peptide ratio extraction, termed MaxLFQ. *Mol. Cell. Proteomics* **13,** 2513–2526
22. Choi, M., Chang, C. Y., Clough, T., Broudy, D., Killeen, T., MacLean, B., and Vitek, O. (2014) MSstats: an R package for statistical analysis of quantitative mass spectrometry-based proteomic experiments. *Bioinformatics* **30,** 2524–2526
23. Benjamini, Y., and Hochberg, Y. (1995) Controlling the False Discovery Rate: A Practical and Powerful Approach to Multiple Testing. *J. R. Stat. Soc. Series B Stat. Methodol.* **57,** 289–300
24. Vizcaíno, J. A., Deutsch, E. W., Wang, R., Csordas, A., Reisinger, F., Ríos, D., Dianes, J. A., Sun, Z., Farrah, T., Bandeira, N., Binz, P. A., Xenarios, I., Eisenacher, M., Mayer, G., Gatto, L., *et al.* (2014) ProteomeXchange provides globally coordinated proteomics data submission and dissemination. *Nat. Biotechnol.* **32,** 223–226